

CHAPTER IV
BLENDS OF CARBOXYLATE ACID POLYMER BASED ON HIGH-DENSITY POLYETHYLENE WITH NYLON

ABSTRACT

Binary polyamide 6 (PA6) and high-density polyethylene (HDPE) blends and ternary PA6/HDPE/Fusabond[®] blends were prepared by melt mixing in a twin screw extruder. Morphology, mechanical properties and thermal behavior were studied over a wide range of compositions. The mechanical properties of PA6/HDPE blend were decreased after melt mixing. The addition of a functionalized high-density polyethylene with maleic anhydride (HDPE-g-MAH, Fusabond[®]) as a compatibilizer resulted in improved mechanical properties as compared with blends without the compatibilizer. In addition, the SEM micrographs show the reduction of dispersed-phase size as the result of adding the compatibilizer, in which the size was reduced to less than 1 μm for both blends of PA6 and HDPE as the dispersed particle. Maximum reduction of the disperse phase size was observed at 1 wt.% compatibilizer. These results could be attributed to chemical reaction between the anhydride groups of HDPE-g-MAH and terminal amine groups of PA 6 in PA6/HDPE/ Fusabond[®] blends. The enhancement of the compatibility of PA6 and HDPE by addition of HDPE-g-MAH was also confirmed through thermal analysis. The decreased in the crystallization temperatures on addition of compatibilizer suggested that there are interactions between PA6 and HDPE-g-MAH occurred in the blend and this retarded the crystallization of the blend components.

Keywords: Polyamide 6, High-density polyethylene, Compatibilizer, Polymer blend, Phase morphology, Mechanical properties, Thermal behavior

INTRODUCTION

As the needs for new and more advanced polymeric materials are growing continuously, the blending of two or more homopolymers is frequently used to fulfill these needs. Polymer blend is a mixture of at least two polymers or copolymers with desirable properties. [1, 2] This method has received increasing attention from both the scientific and industrial communities as they afford an attractive low-cost substitute to the development of entirely new materials. Most industrial polymer blends are incompatible. Blending of them leads to exhibition of two-phased separation that consist of one of components plays as the continuous matrix and the another component as a dispersed phase. Hence, the final blend properties are affected by controlling and stabilizing the blend morphology. The achievement of compatibilization, whether by addition of a third component that is called compatibilizer or by in situ chemical reaction between blend components, a so-called reactive blending will help to improve the blend properties. [1, 2] The role of compatibilizer is similar to that of an emulsifier in classical emulsion technology. Compatibilizer should migrate to the interface causing reduction of dispersed phase dimensions and stabilization of blend morphology.

The polyamide 6 (PA6)/Polyethylene (PE) blend has received much attention become blends of these two materials lead to the combination of the desirable properties of both polymer. Polyamide 6 is the most widely used engineering plastic with good mechanical properties, weather and thermal resistant and good oxygen barrier, while PE has high impact strength and good moisture barrier. The different types of PE were blended with polyamide (such as UHMWPE [3], LLDPE [10, 11], LDPE [4-9], and HDPE [12-16]). However, these blends are immiscible blends due to the presence of polar groups in the PA6 and the non-polar ones of PE. Miscibility of these blends were improved by adding block, graft copolymer [7, 8, 13], adduct of maleic anhydride [3, 5, 10, 11], terpolymer such as ethylene/butylacrylate/maleic anhydride terpolymer [19], and ethylene/methacrylic acid/isobutylacrylate terpolymer [9, 14, 16]. According to these articles, the results showed that there were the reduction of the size of dispersed phase and the stabilization of phase morphology in the blends.

In this work, the effect of maleic anhydride grafting on high-density polyethylene as a compatibilizer on the morphology, thermal behavior, and mechanical properties in PA 6 / HDPE blends were studied.

EXPERIMENTAL

Materials

Polyamide 6 employed in this study was an injection-molding grade (1013B), supplied by UBE nylon (Thailand). The HDPE was also an injection-molding grade (H54805) supplied by Thai polyethylene Co., Ltd. Finally, HDPE-g-MAH under the trademark Fusabond[®] E MB 100D (0.9 wt% MAH graft level), was supplied by DuPont, USA.

Blend preparation

All the components were dried in a hot-air oven for at least 12 hours at 60°C to remove moisture prior to use. Binary PA6/HDPE and ternary PA6/HDPE/HDPE-g-MAH blends were melt blended in a Model T-20 corotating twin-screw extruder (Collin) with $L/D=30$ and $D=25$ mm; the processing conditions were the following: temperature (°C): 75, 200, 215, 220, 220, and 230 from hopper to die, respectively and screw rotation (rpm): 35. The binary PA6/HDPE blends were prepared with weight ratios of 80/20, 60/40, 50/50, 40/60, and 20/50. When a compatibilizer was employed, 0.1-35 parts of it were added to 100 parts of the blends. Each of compositions was premixed in a tumble mixer before introducing into the twin-screw extruder to be mixed and extruded through a single strand die, and solidified with cold water (temperature 35°C) and pelletized. The pellet obtained were dried in a hot-air oven for at least 12 hours at 60°C and kept in the sealed plastic bags, prior to compression molding. So that the moisture regain at the blends would be minimized.

Specimen Preparation

Test specimens were prepared using a Wabash V 50 H 50-ton compression-molding machine. The pellets were placed in a picture frame mold and the mold was preheated at 240°C for 3 minutes in the press without any applied pressure for complete melting. The mold was then compressed under a force of 10 tons for a further 3 minutes after which the mold is cooled to 40°C under pressure. Test specimens were cut from the molded sheets using a pneumatic die cutter.

Phase Morphology

Scanning electron microscope (SEM), JEOL 5200-2AE (MP152001) was used to study phase morphologies of the blends. The specimens were fractured in liquid nitrogen and etched using (i) hot decalin (for HDPE minor phase blends) and (ii) formic acid (for PA6 minor phase blends). The specimens were then coated with gold under vacuum. All SEM studied were characterized using magnification of 750 and 1500 times at 20 kV.

Thermal analysis

Thermal analysis of the blends was carried out under nitrogen gas atmosphere on samples weighting about 7-10 mg, using a Perkin-Elmer DSC 7 instrument. The thermograms were obtained by heating of samples from 30°C to 250°C at a heating rate of 80°C/min, held for 5 min at this temperature in order to cancel any thermal and processing history, and then cooled from 250°C to 30°C at a cooling rate of 10°C/min. The samples were heated again from 30°C to 250°C at a heating rate of 10°C/min. The recorded temperatures were calibrated using Indium as standard.

Fourier Transform Infrared Spectrometry (FTIR)

FTIR spectra of the blends were obtained from film samples. These film samples were prepared using a compression-molding machine. Fourier Transform Infrared Spectrophotometer (FTIR) was used to probe the specific interpolymer interactions between Fusabond[®] and the blends. Measurements were made in absorbance mode using a Bruker FTIR Spectrometer, model Vector 3.0, using 32 scans at a resolution of 4 cm⁻¹.

Molau test

Molau test was a solubility test that was used to determine the formation of copolymer formation in PA6/HDPE blends. [11] The test was carried as following 0.1 gram of sample was added to 5 ml of 80% formic acid. The mixture was shaken for 10 minutes and then allowed to stand for blends without copolymerization, the

solution obtained will be phase solution (PA6 soluble in formic acid and HDPE does not). For blends with copolymerization, a persistence turbid will be observed.

Mechanical and Physical Properties Testing

Tensile properties, impact property and hardness of the blends were determined from the compressed specimens following the test conditions suggested by ASTM.

An Instron Universal testing machine was used to measure the tensile strength and tensile modulus of the blends. The tests were conducted according to ASTM D638-91 test procedure, using a crosshead speed of 50 mm.min⁻¹. Izod impact strength was measured using a Zwick Impact tester according to ASTM D 256-92 test procedure method with a 2.7 J pendulum. Rockwell hardness tester (Matsuzawa DXT) was used to measure hardness of the blends. The test was conducted according to, ASTM D785 test procedure.

All the tests were done at room temperature (30°C) and the results were obtained from the average of ten specimens for each blend ratio.

RESULTS AND DISCUSSION

Phase morphology

The SEM micrographs of fracture surfaces of uncompatibilized blends are shown in Figure 1. These micrographs clearly show that the dispersed phase particle is the spherical in shape in the polymer matrix. In the blend of PA6/HDPE, which contained high PA6 content (HDPE was the dispersed phase) larger dispersed particle size when compared to the blend, which contained high HDPE content (PA6 was the dispersed phase) were observed. Presumably a larger HDPE dispersed phase was found because the viscous force which attempt to break the drop was much lower for HDPE in PA6 matrix than for PA6 in HDPE matrix. The micrographs of the compatibilized PA6/HDPE blends are shown in Figures 2 and 3. When the small amount of the compatibilizer (0.1 wt.%) was added. It resulted in decrease of the dispersed particle size and for both HDPE and PA6 as a dispersed phase. However, the homogeneity of the dispersed phase size of the blend was not observed until the 2.5 wt.% of the compatibilizer was added. The reduction of dispersed phase size when the compatibilizer was added, was due to the ability of the compatibilizer to reduce the interfacial tension between the dispersed phase and the matrix phase. The reduction of the interfacial tension could be caused by the chemical interaction between the terminal amine group in PA6 and the maleic anhydride functional group in the compatibilizer increased the interfacial adhesion of the blend.

The number average size of the particle diameter of dispersed phase of the compatibilized blends is reported in Figure 4. It was found that the dispersed phase sizes decreased to less than 1 μm for both blends of HDPE and PA6 as a dispersed phase by the addition of the compatibilizer. In addition, in all cases, it appeared that approximately 1 wt.% of the compatibilizer is sufficient to produce maximum reduction of the dispersed particle diameter. No further decreased in dispersed particle sizes were observed when more compatibilizer was added.

Fourier transform infrared spectrometry

One possible chemical interaction in PA6/HDPE/Fusabond[®] blend that could take place during melt mixing is imidization formation between terminal amine groups of PA6 and anhydride groups of Fusabond[®] at the interface. As suggested by Ide and Hasegawa in 1994 (see Figure 5).

FTIR spectra of PA6/HDPE blends with and without compatibilizer are shown in Figure 6. For pure PA6 (Fig.6a), the characteristic peaks were observed at 3300 and 3068 cm^{-1} , which corresponded to the N-H stretching of primary amides. C-H stretching peak at 2930 and 2865 cm^{-1} . And peaks at 1643 and 1544 cm^{-1} correspond to C=O stretching and N-H bending were also observed. For pure HDPE (Fig.6d), the characteristic peaks are 2917 and 2851 cm^{-1} corresponded to the C-H stretching. The peak at 1465 cm^{-1} represents $-\text{CH}_2$ group. Spectra of the uncompatibilized blend (Fig.6b) show all the characteristic peaks of both pure PA6 and pure HDPE. However, for the compatibilized blend (Fig.6c) An additional peak at 1671 cm^{-1} , which was not present in the spectra of pure PA6 and pure HDPE. This peak belong to C=O, amide I [20]. From FTIR spectra, they indicate that there were chemical reactions between terminal amine groups of PA6 and anhydride groups of HDPE-g-MAH in the blend.

The copolymerization formation was confirmed by the Molau test. The results of the Molau test are shown in Figure 7. After several hours, the bottle containing the pure PA6 (as a control) (Fig.7a) shows a persistent clear solution because pure PA6 was dissolved in formic acid. For the bottle containing binary PA6/HDPE blend (Fig.7b) shows the phase separation that consisted two distinguish phases of the lower part of the solution, which was PA6 dissolved in formic acid and the upper part, which was HDPE component that did not dissolve in formic acid. The persistently turbid solution is observed in the bottle containing ternary blend of PA6/HDPE/Fusabond[®]. The formation of colloidal suspension in the Molau test indicated that the grafting copolymer had taken place.

FTIR results together with Molau test results confirmed that there were interactions between the terminal amine groups of PA6 and the anhydride groups of the Fusabond[®] to give amide groups.

Mechanical properties

The tensile modulus of the uncompatibilized PA6/HDPE blends is shown in Figure 8. The tensile modulus of these blends decreased as the HDPE content increased, as compared with that of pure PA6. In general, the tensile modulus of immiscible blends is dependent on the modulus and crystallinity of the polymer constituting the continuous phase. The amide groups in the PA6 molecular chains provide PA6 with higher rigidity than HDPE, which molecular chain contains only ethylene repeating units. The rigid constituent in the molecular chain of PA6 would give higher tensile modulus when compared to HDPE. Therefore, adding HDPE to the blend, as the HDPE content increases, would result in the reduction of tensile modulus of the blend. In addition, the compatibility and the phase morphology also affect the tensile modulus of immiscible blends. Therefore, the lack of compatibility and coarse phase morphology of the PA6/HDPE blends would result in decreased tensile modulus of the uncompatibilized blends. The increase in tensile modulus of PA6/HDPE blends is observed with the addition of the compatibilizer (Fig. 9). When a small amount of compatibilizer (0.1-1.0 wt.%) was added, the tensile modulus values of the compatibilized blends gradually increased as compared with the uncompatibilized blends. This behavior was due to the chemical interaction between the compatibilizer and PA6, which was mentioned earlier in the FTIR results. This interaction has improved the compatibility of the PA6/HDPE blend. And also the result of the reduction of dispersed phase size was observed in the SEM results. As far as the addition of compatibilizer was more than 2.5 wt.%, the tensile modulus values of the compatibilized blends are much higher than that of the uncompatibilized blends. This feature can be explained that when more than 2.5 wt.% of compatibilizer was added, not only the improvement of compatibility of the blends and the reduction of dispersed phase size were observed, but also the homogeneity of dispersed phase size in the blends was improved. However, the tensile modulus of all the blends was decreased with the amount of compatibilizer greater than 10 wt.%. This could be affected by the substantial reduction of crystallinity of the continuous phase as compared with neat polymer. Tensile modulus of PA6/HDPE/Fusabond[®] (80/20/10) blend was 1.43 times higher than that of the blend of PA6/HDPE (80/20).

Figure 10 shows the plot of tensile strength versus wt.% of HDPE contents of uncompatibilized PA6/HDPE blends. The tensile strength of these blends is lower than that of pure material. In particular, tensile strength of the uncompatibilized blends is decreased with increasing HDPE contents. This is because of the rigid parts on the PA6 molecular chain give higher tensile strength than HDPE. In addition, the reduction of tensile strength of the blends could also be due to the poor interfacial adhesion between two phases, which resulted in the weak stress transfer from one phase to another phase. Furthermore, the dispersed phase in the matrix also leads to the presence of stress concentrations that give a weak point in the blends. Tensile strengths of the PA6/HDPE blends are enhanced by the addition of the compatibilizer as shown in Figure 11. These values are gradually increase when the amounts of compatibilizer increase. This indicated that compatibilizer improves the interfacial adhesion and causes the dispersed particle size to decrease resulting in better stress transfer between two phases were occurred. Nevertheless, when more than 10 wt.% of compatibilizer was added, the tensile strength values of the blends are decreased. Tensile strength of the PA6/HDPE/Fusabond[®] (80/20/10) blend was approximately 1.35 times higher than that of the blend (80/20 PA6/HDPE).

The impact strengths of uncompatibilized PA6/HDPE blends versus the HDPE content are shown in Figure 12. From the plot it can be clearly seen that impact strength of uncompatibilized blends increased as the HDPE content increased. This could be due to the incorporation of HDPE, which has more entanglement from its branch segment, required more energy to remove the entangled molecular chain. Also, when the addition of compatibilizer in the PA6/HDPE blends, the impact strength is slightly increased as shown in Figure 13. The impact strength values of compatibilized blends (80/20 PA6/HDPE) are about 1-3 times higher than that of uncompatibilized blends. This improvement can also explain by the improved interfacial adhesion, which allow adsorbed energy to transfer from one phase to another phase.

The hardness of the PA6/HDPE blend with and without compatibilizer was shown in Figures 14 and 15, respectively. The hardness of neat PA6 is higher than that of neat HDPE. This indicates that the PA6 is harder than HDPE due to the molecular chain of PA6 was more tightly packed than HDPE. Therefore, the

hardness of the uncompatibilized PA6/HDPE blend is decreased as the amount of HDPE content increased. This result could be supported from the crystallinity of the PA6 in the blend decreased as the HDPE content increased (see DSC result). When the small amount of compatibilizer (0.1-2.5 wt.%) in the PA6/HDPE blends increased, the hardness of the blends is increased. Hardness of compatibilized PA6/HDPE blend (80/20) is 1.05-1.09 times higher than that of the uncompatibilized blends. This implied that the compatibility of the PA6/HDPE blends is improved by addition of Fusabond[®] as a compatibilizer. At large amount of compatibilizer (5-35 wt.%), the compatibilizer played an important role in trivial improved the hardness of the blend until reached the plateau.

Differential scanning calorimetry

Effect of compatibilizer on the melting and crystallization temperatures and weight fraction crystallinity of each component of the blends were studied.

Figure 16 shows DSC exothermic thermograms of PA6/HDPE blends. The crystallization temperature (T_c) peak of pure PA6 and pure HDPE occurred at 189.8°C and 119.3°C, respectively. No change in T_c of the HDPE component in the PA/HDPE blends was observed. On the other hand, T_c of PA6 component is barely discernible higher than T_c of pure PA6. It is possible that the phase boundary interface between PA6 and HDPE phases behaves as a nucleation site for PA6. DSC exothermic thermograms of PA6/HDPE blends at various compatibilizer contents are shown in Figures 17 and 18. In PA6/HDPE 80/20 blends (Fig.17), the addition of compatibilizer resulting in a slight decrease in the T_c peak of both PA6 and HDPE components as compared with the neat polymer. This indicated that the presence of compatibilizer in the blends retarded the crystallization of each component. In addition, for PA6/HDPE 20/80 blends (Fig 18), the effect of addition of compatibilizer on the T_c peak of PA6 and HDPE components is relatively similar to that of the PA6/HDPE 80/20 blends. However, at the compatibilizer rich blend (2.5-35%wt.), the T_c peak of PA6 component could not be observed.

Figure 19 shows DSC melting thermogram of PA6/HDPE blends without compatibilizer. Thermogram of the pure PA6 shows the two melting temperatures

(T_m) at the shoulder peak 217°C and the sharp peak 225°C. These two melting temperatures have been reported that they represent the two kinds of crystal structure in polyamide, the melting temperature at 217°C corresponds to γ -form, and the melting temperature at 227°C corresponds to α -form [17]. For the pure HDPE, the T_m peak occurs at 135.5°C. The T_m peaks of each component in the PA6/HDPE blends are not difference from both neat polymers.

Melting thermograms of PA6/HDPE blends with compatibilizer are reported in Figures 20 and 21. The addition of compatibilizer resulting in lowering the T_m peak of both PA6 and HDPE components when compared with both pure polymers. However, in the HDPE-rich blend (PA6/HDPE 20/80) (Fig.21), when the amount of compatibilizer added higher than 2.5 wt.%, the γ -form melting temperature peak of PA6 was not observed.

For the weight fraction crystallinity (χ_c) of PA6 and HDPE components of PA6/HDPE blend with and without compatibilizer is presented in Tables 1. All the composition ratios of uncompatibilized blends showed that the weight fraction crystallinity for both PA6 and HDPE components was less than both pure polymers. This implied that the crystallization of one component was affected by the addition of another component. However, the χ_c of PA6 component is significantly dependent on compatibilizer content, this value decreased slightly as amount of compatibilizer content increase when compared with pure PA6. On the contrary, the χ_c of HDPE component dramatically increased when amount of compatibilizer increase with respect to the pure polymer. It is possible that the ethylene segments from the compatibilizer can co-crystalline with ethylene segments from HDPE because there was no indication of a separate compatibilizer endotherm in the DSC melting thermogram of compatibilized PA6/HDPE blends (Fig. 20 and 21). Table 2 summaries the melting and crystallization temperatures of pure polymers and PA6/HDPE blends with and without compatibilizer.

CONCLUSIONS

The SEM micrographs of uncompatibilized PA6/HDPE blend showed the coarse phase morphology of dispersed phase in the continuous phase over a wide

range of composition as a result of the weak interfacial adhesion between two phases. This resulted in poor mechanical properties. The addition of Fusabond[®] as a compatibilizer in the PA6/HDPE blend enhanced the compatibility of PA6/HDPE blend due to the interactions between the terminal amine groups of PA6 and the anhydride groups of compatibilizer. These interactions could be confirmed by the FTIR result. The improvement of compatibility of the PA6/HDPE blend had resulted in reduction of size of dispersed phase less than 1 μm . Maximum reduction of dispersed phase size was observed at compatibilized blend with 1 wt.% of Fusabond[®]. The enhancement of mechanical properties of the PA6/HDPE blend was also observed. The maximum improvement of the tensile properties was observed at compatibilized blend with 10 wt.% of Fusabond[®]. Tensile modulus and the tensile strength of the compatibilized PA6/HDPE blend (80/20) (10 wt.% Fusabond[®]) were 1.43, 1.35 times that value of the uncompatibilized blend. Impact strength of the compatibilized PA6/HDPE (80/20) blend was 1-3 times that of the uncompatibilized PA6/HDPE blend. At the small amount of the compatibilizer (0.1-2.5 wt.%), the hardness of the compatibilized PA6/HDPE (80/20) blend was also 1.05-1.09 times higher than the uncompatibilized blend. Moreover, the decrease in the crystallization temperatures, the melting temperatures and crystallinity of each component in the blends as compared with both pure PA6 and HDPE supported that the compatibility of the PA6/HDPE blend was improved by adding Fusabond[®] as a compatibilizer.

ACKNOWLEDGMENTS

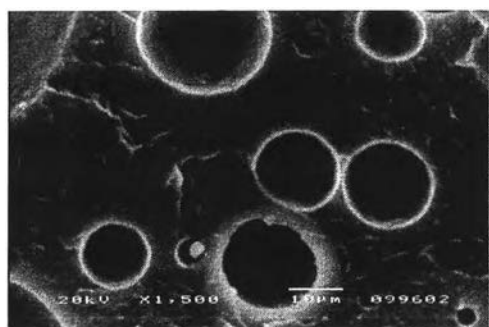
Authors are thankful to DuPont company (U.S.A.), TPE Co.,Ltd., and UBE nylon (Thailand), for providing the materials for carrying out the present work.

REFERENCES

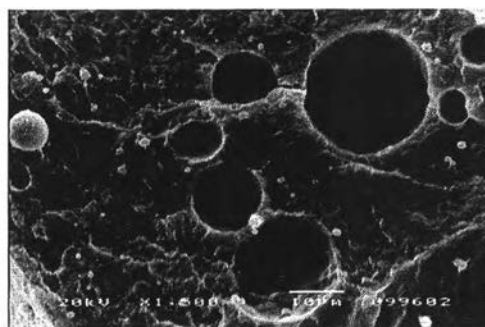
1. Folkes, M.J., and Hope, P.S., Polymer blends and alloys. London: blackie academic & professional, (1993).
2. Utracki, L.A., Polymer alloys and blends. Munich, Hanser, (1991).
3. Yao, Z., Yin, Z., Sun, G., liu, C., Tong, j., Ren, L., and Yin, J., J. Appl. Polym. Sci., 70, 232 (2000).

4. Gary, F., and Robert, E.P, Polym. Eng. Sci., 27(20), 1495 (1987).
5. Cuihong, J., Sara, F., and Pierluigi, M., Polymer, 44, 2411 (2003).
6. Macknight, W.J., and Lenz, R.W., Polym. Eng. Sci., 25, 1124 (1985).
7. Everaldo, F.S., and Bluma, G.S., J. Appl. Polym. Sci., 60, 1687 (1996).
8. Asa, H., Mehrnoush, J.D., and Bengt, W., Polymer, 42, 8743 (2001).
9. Leewajanakul, P., Pattanaolarn, R., Ellis, J.W., Nithitanakul, M., Grady, B.P., J. Appl. Polym. Sci., 89, 620 (2003).
10. Kudva, R.A., Keskkula, H., and Paul, D.R., Polymer, 40, 6003 (1999).
11. Valdes, S.S., Flores, I.Y., Valle, L.F.R., Fernandez, O.S.R., Villarreal, F.O., and Quintanilla, M.L., Polym. Eng. Sci., 38, 127 (1998).
12. Fellahi, S., Favis, B.D., and Fisa, B., Polymer, 37, 2615 (1996).
13. Serpe, G., Jarrin, J., and Dawans, F., Polym. Eng. Sci., 30, 553 (1990).
14. Chen, C.C., and White, J.L., Polym Eng. Sci., 33, 923 (1993).
15. Chen, C.C., Fonpan, E., Min, K., and White, J., Polym. Eng. Sci., 28, 69 (1988).
16. Willis, J.M., and Favis, B.D., Polym. Eng. Sci., 28, 1416, (1988).
17. Psarski, M., Pracella, M., and Galeski, A., Polymer, 41, 4923 (2000).
18. Ide, F., Hasegawa, A., J. Appl. Polym. Sci., 18, 963 (1974).
19. Beltrame, P.L., Castelli, A., Pasquantonio, M.D., Canetti, M., and Seves, A., J. Appl. Polym. Sci., 60, 579 (1996).
20. Ghosh, M.K., and Mittal, K.L. Polyimides fundamentals and application, New York, (1996).

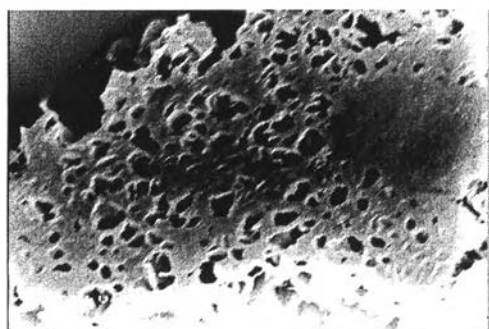
Figure 1 The SEM micrographs of blends without Fusabond[®] as compatibilizer at the following PA6/HDPE ratios: (a) 80/20, (b) 60/40, (c) 50/50, (d) 40/60, (e) 20/80.



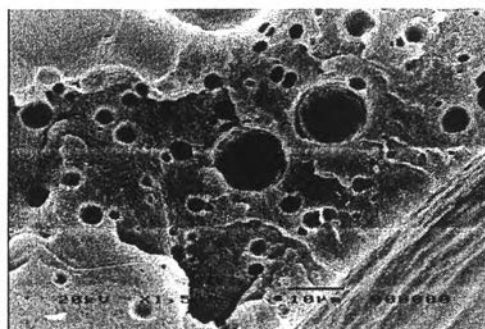
(a)



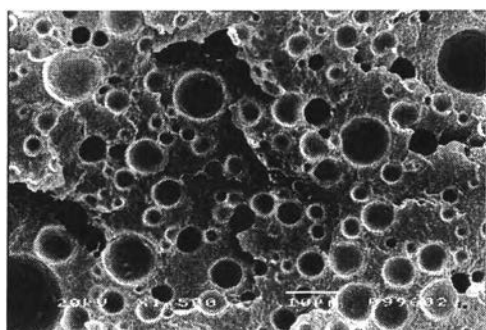
(b)



(c)

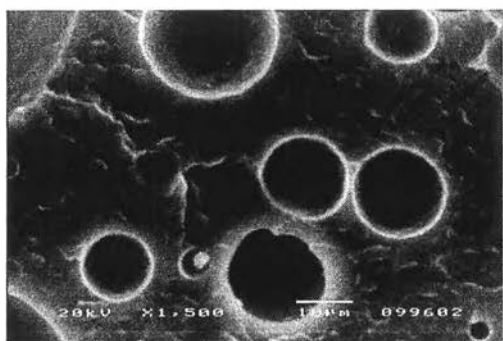


(d)

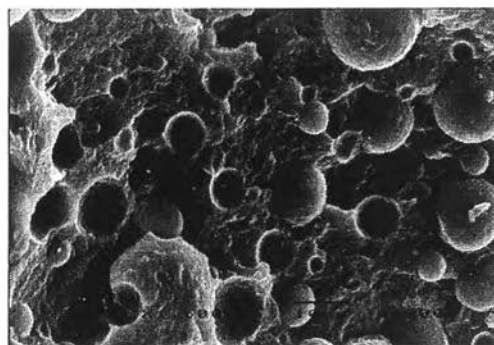


(e)

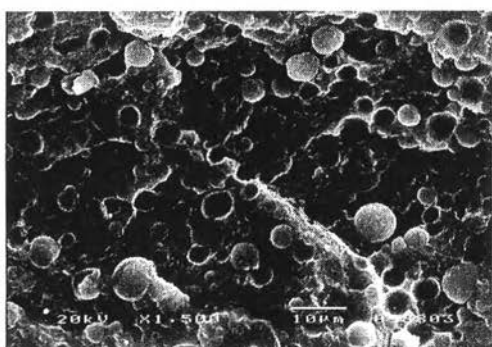
Figure 2 The SEM micrographs of 80/20 PA6/HDPE blends with added Fusabond[®] compatibilizer at the following weight percentages: (a) 0, (b) 0.1, (c) 0.5, (d) 1.0, (e) 2.5, and (f) 35%.



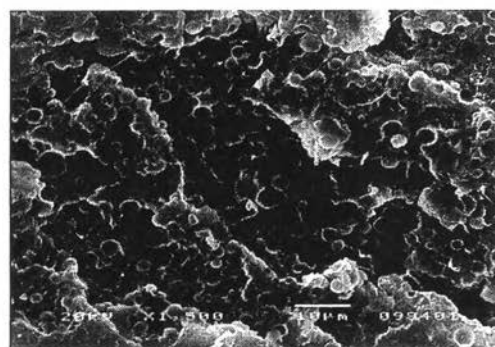
(a)



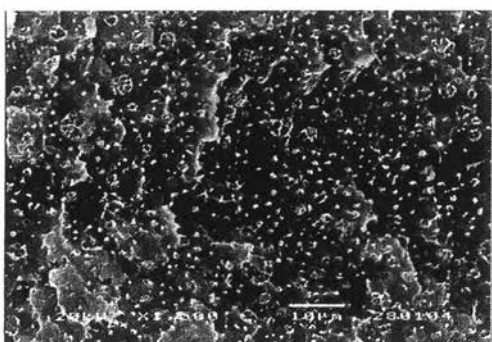
(b)



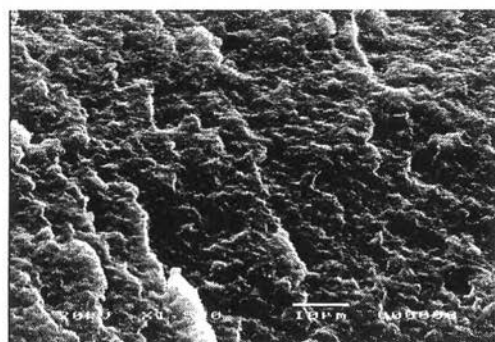
(c)



(d)



(e)



(f)

Figure 3 The SEM micrographs of 20/80 PA6/HDPE blends with added Fusabond[®] compatibilizer at the following weight percentages: (a) 0, (b) 0.1, (c) 0.5, (d) 1.0, (e) 2.5, and (f) 35%.

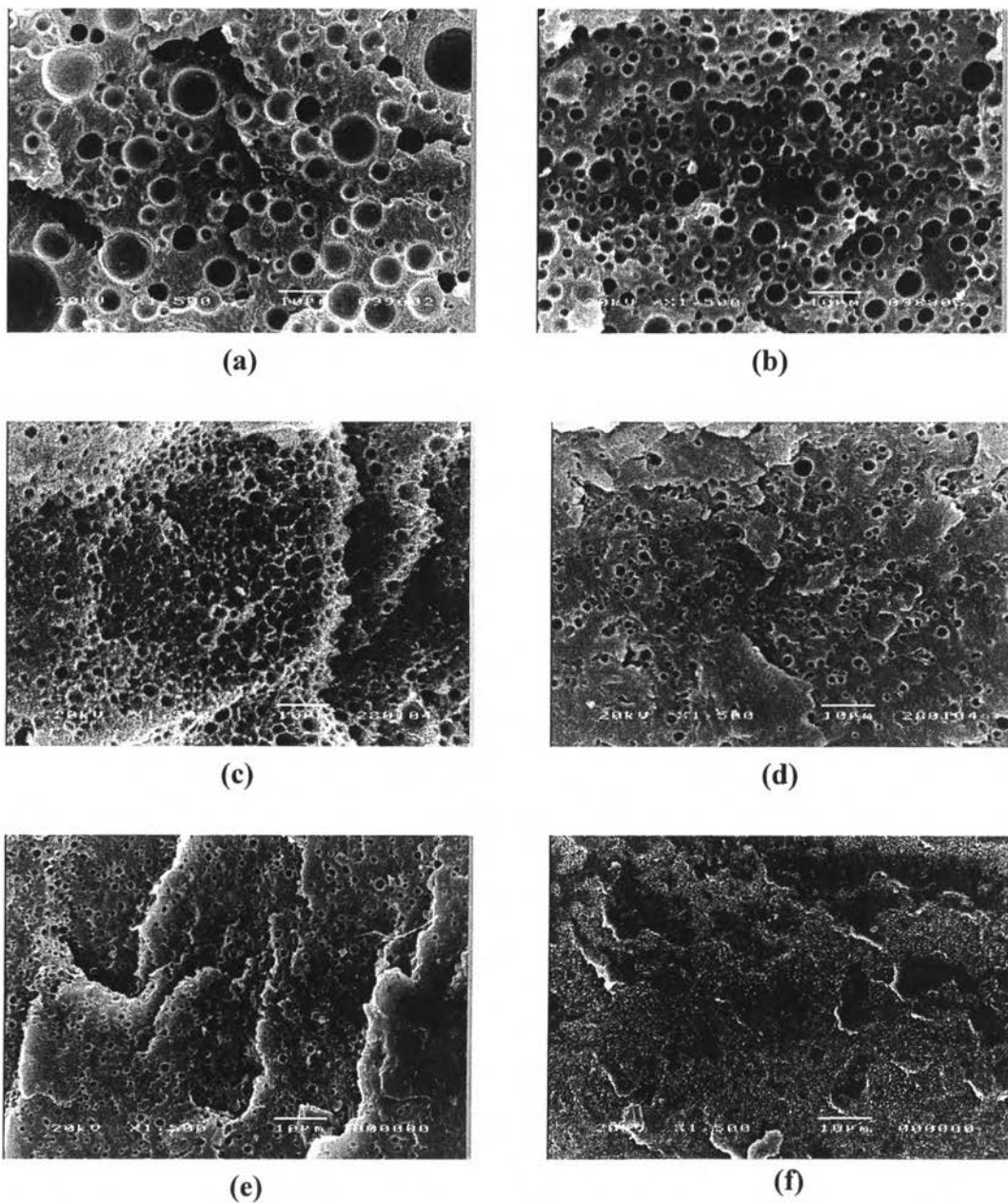


Figure 4 The number average particle diameter of dispersed phase of PA6/HDPE as a function of Fusabond[®] content.

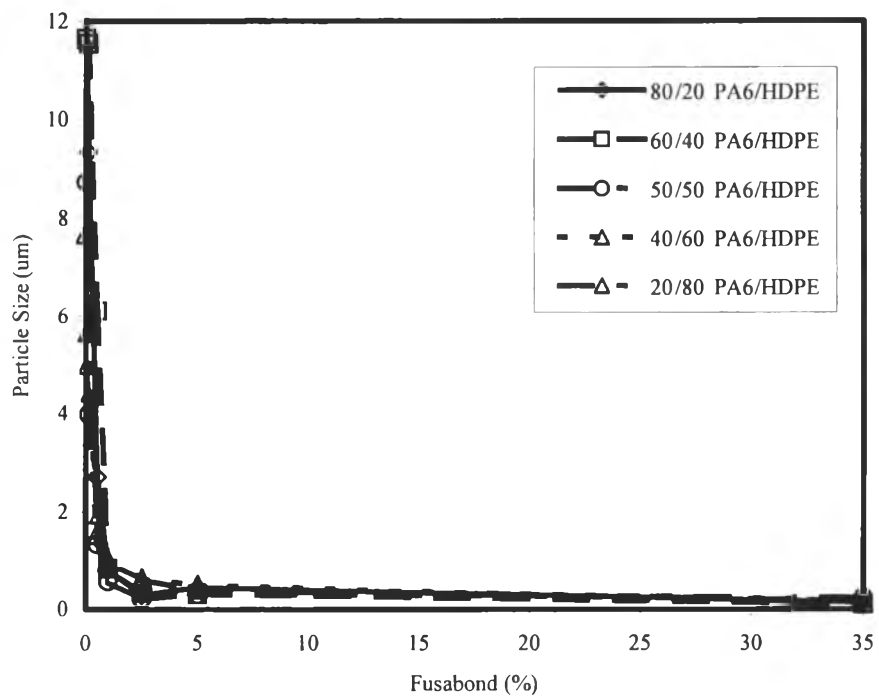


Figure 5 The chemical interaction between PA6 and Fusabond[®] as a compatibilizer.

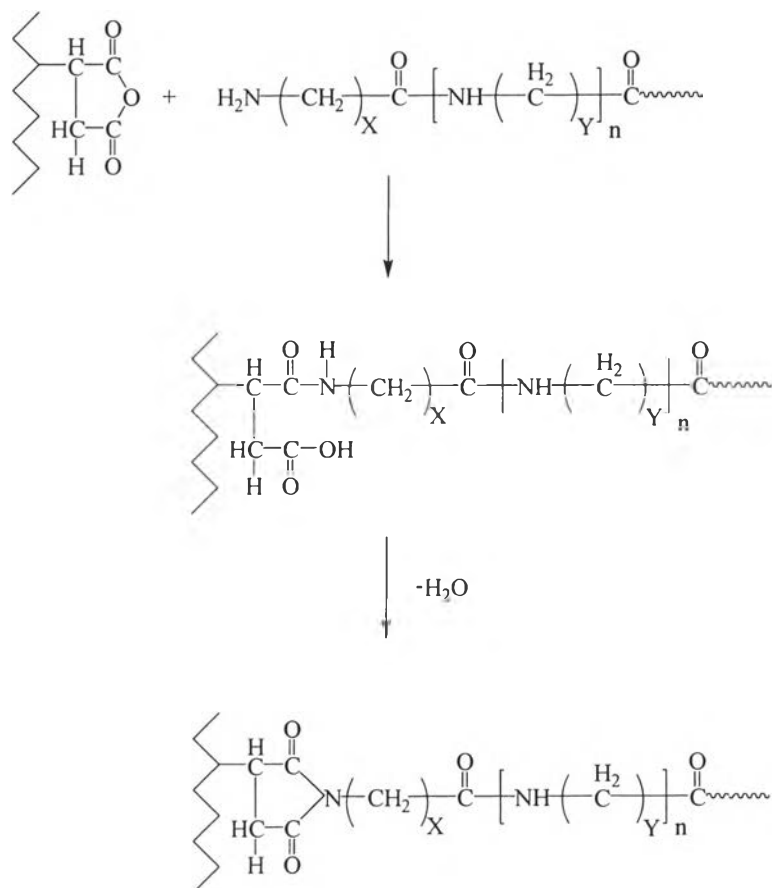


Figure 6 FTIR spectra of (a) pure PA6, (b) compatibilized blend, (c) uncompatibilized blend, and (d) pure HDPE.

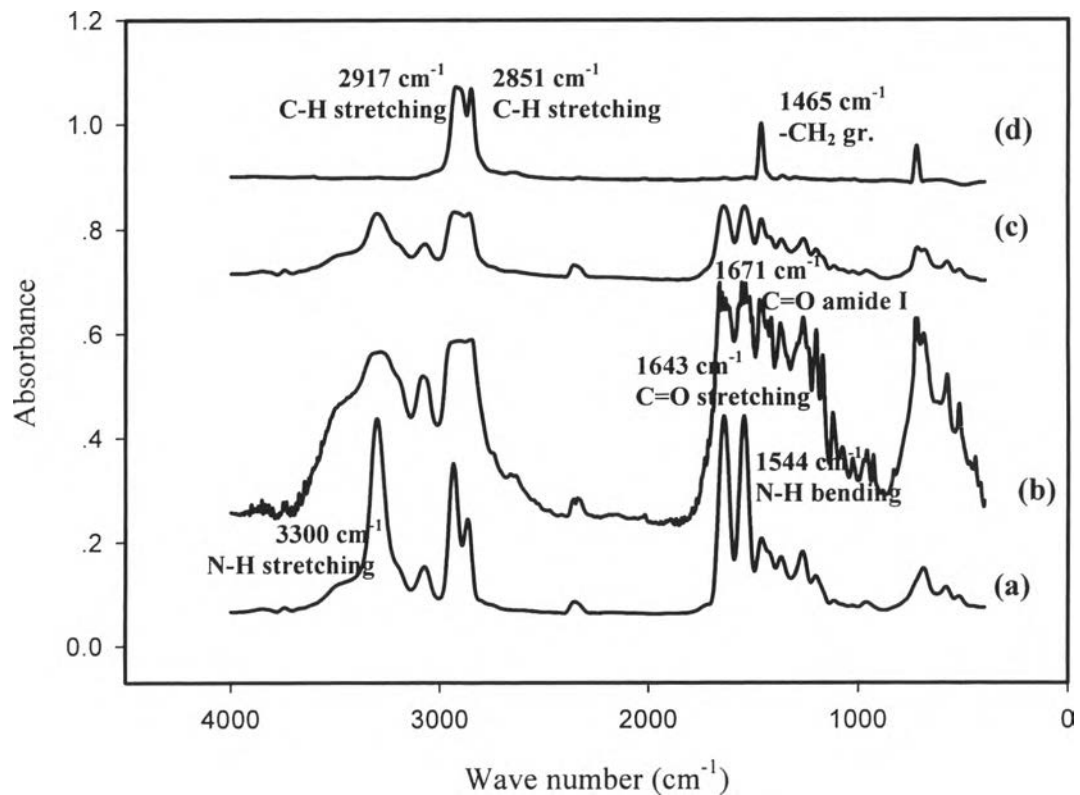


Figure 7 The molau test of (a) pure PA6, (b) uncompatibilized blend, and (c) compatibilized blend.

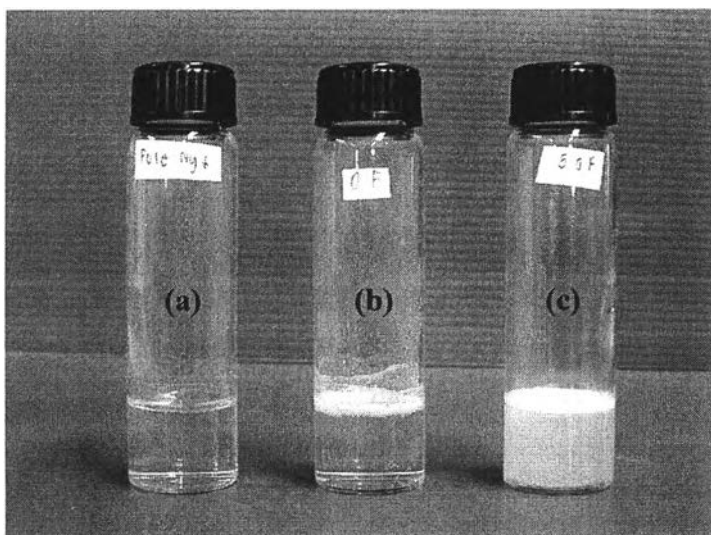


Figure 8 Tensile modulus of uncompatibilized PA6/HDPE blends.

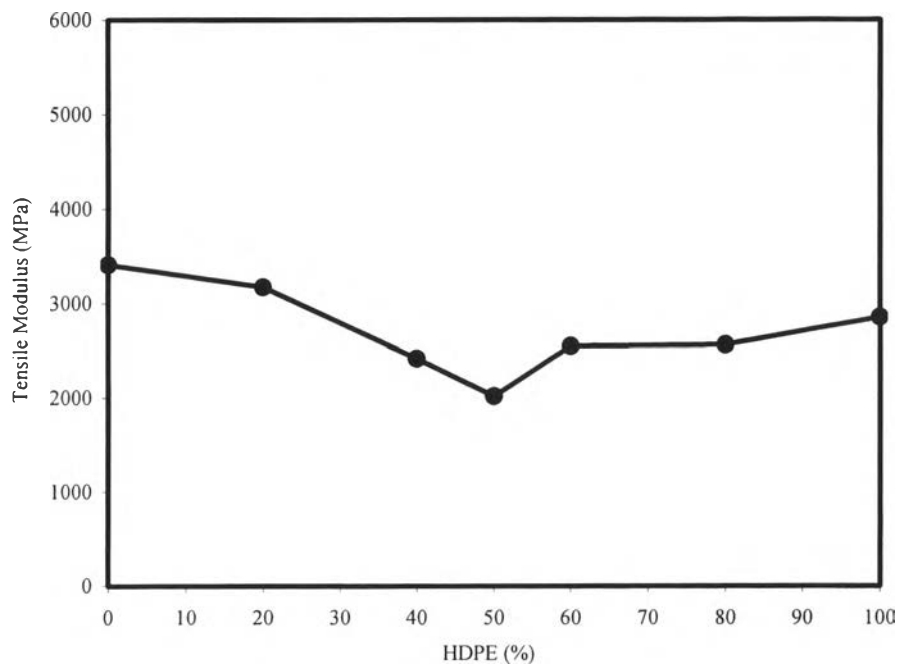


Figure 9 Tensile modulus of PA6/HDPE blends as a function of Fusabond[®] content.

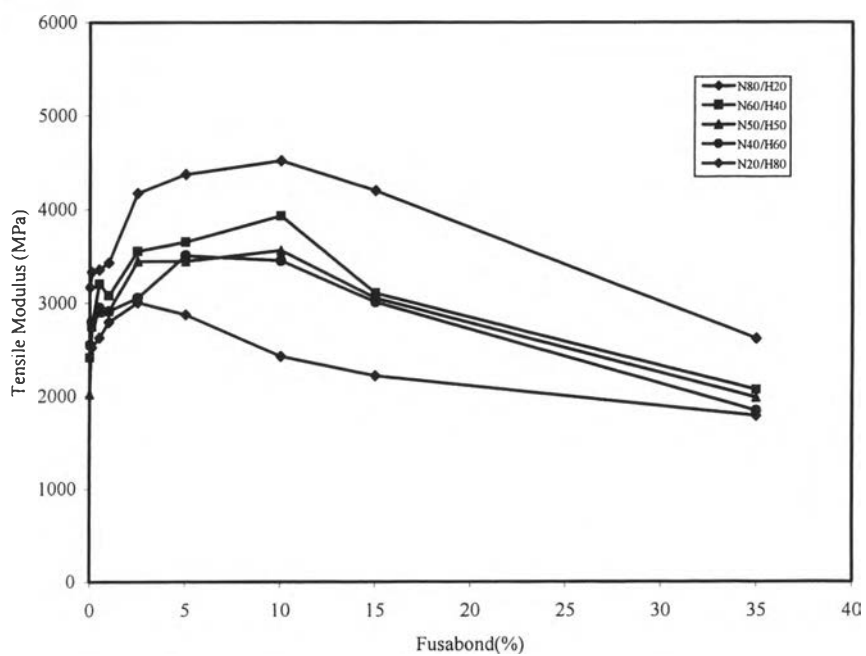


Figure 10 Tensile strength of uncompatibilized PA6/HDPE blends.

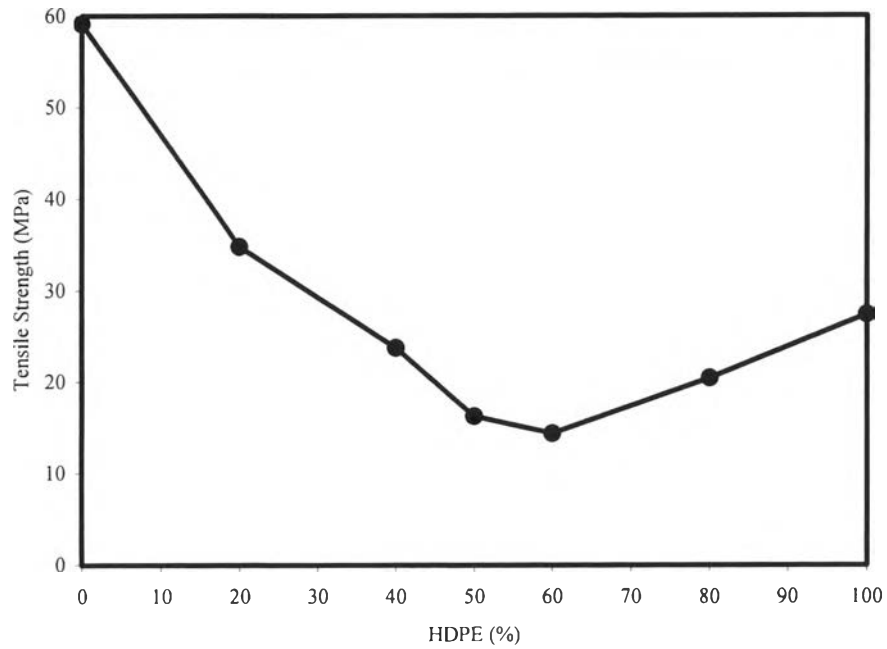


Figure 11 Tensile strength of PA6/HDPE blends as a function of Fusabond[®] content.

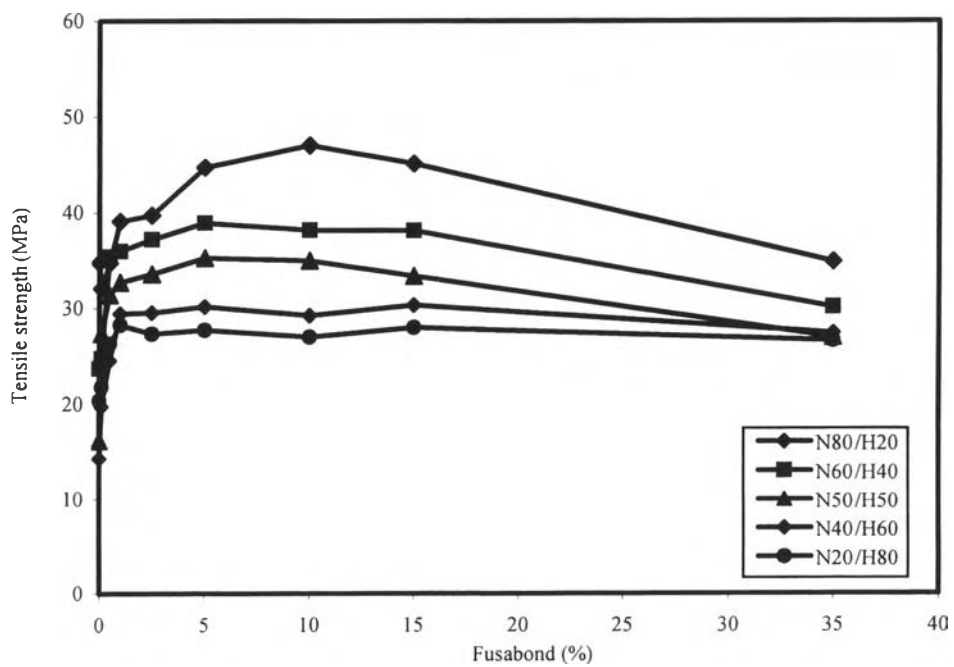


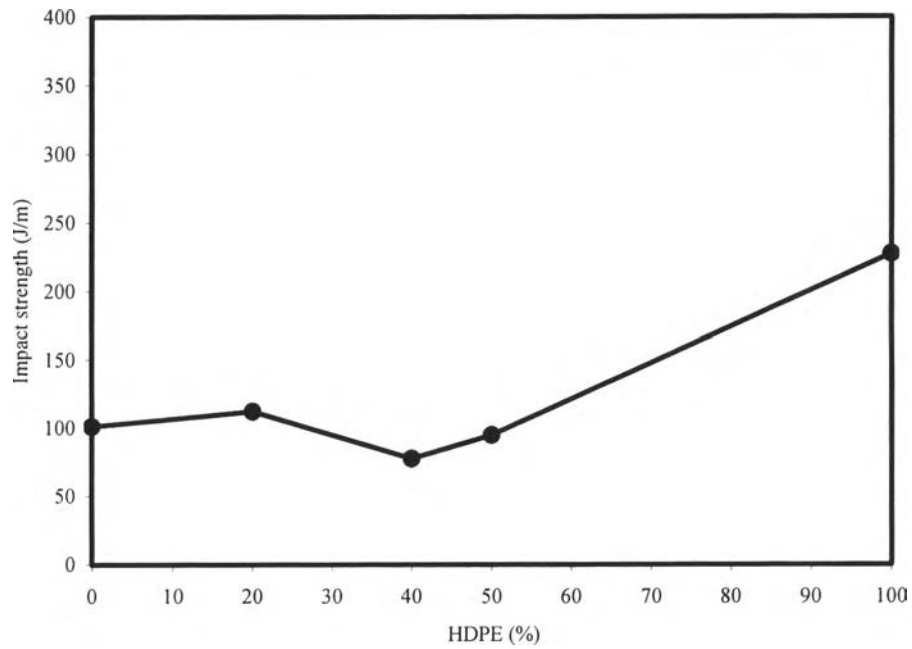
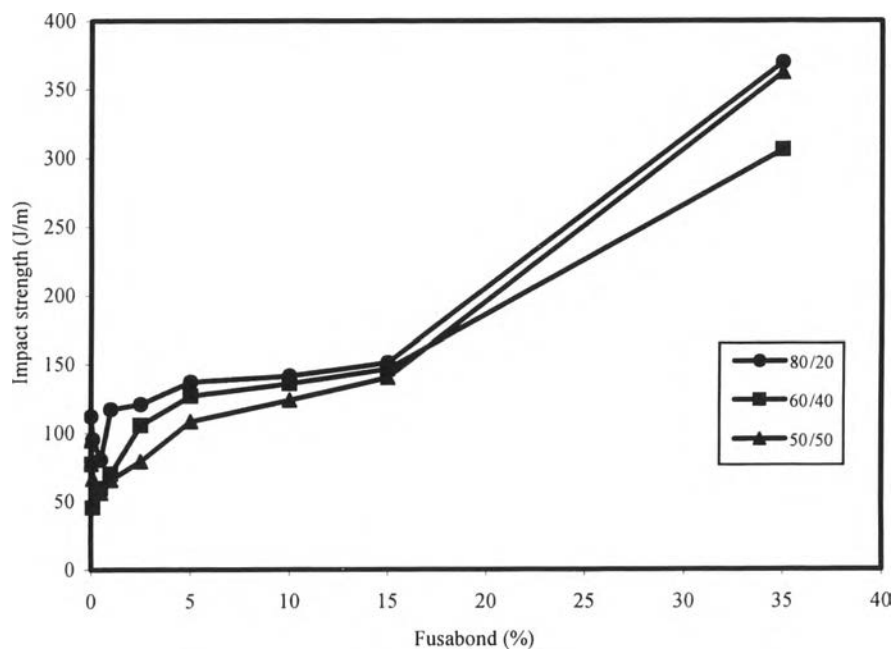
Figure 12 Impact strength of uncompatibilized PA6/HDPE blends.**Figure 13** Impact strength of PA6/HDPE blends as a function of Fusabond[®] content.

Figure 14 Hardness of uncompatibilized PA6/HDPE blends.

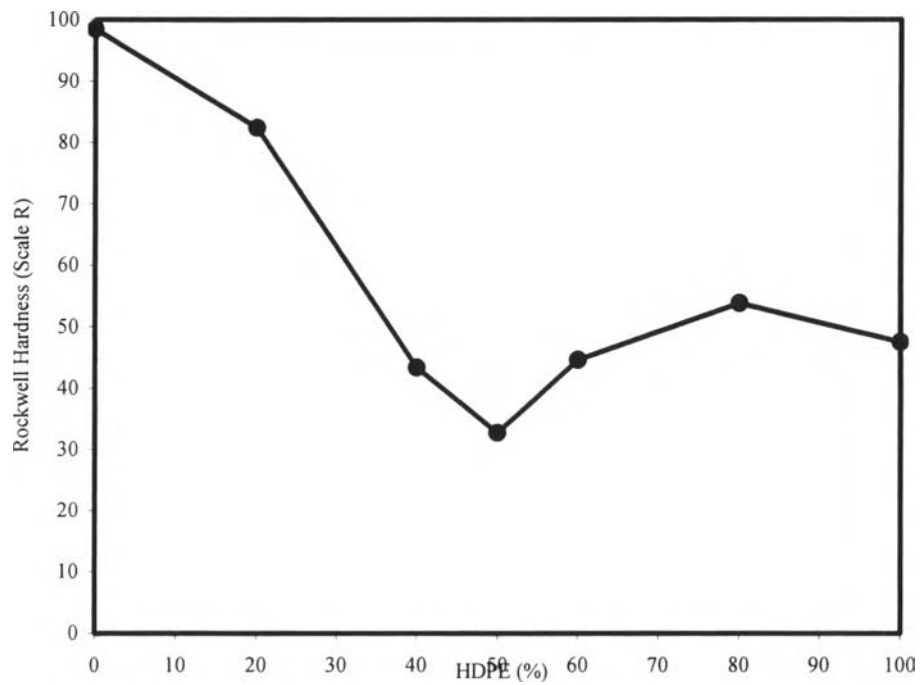


Figure 15 Hardness of PA6/HDPE blends as a function of Fusabond® content.

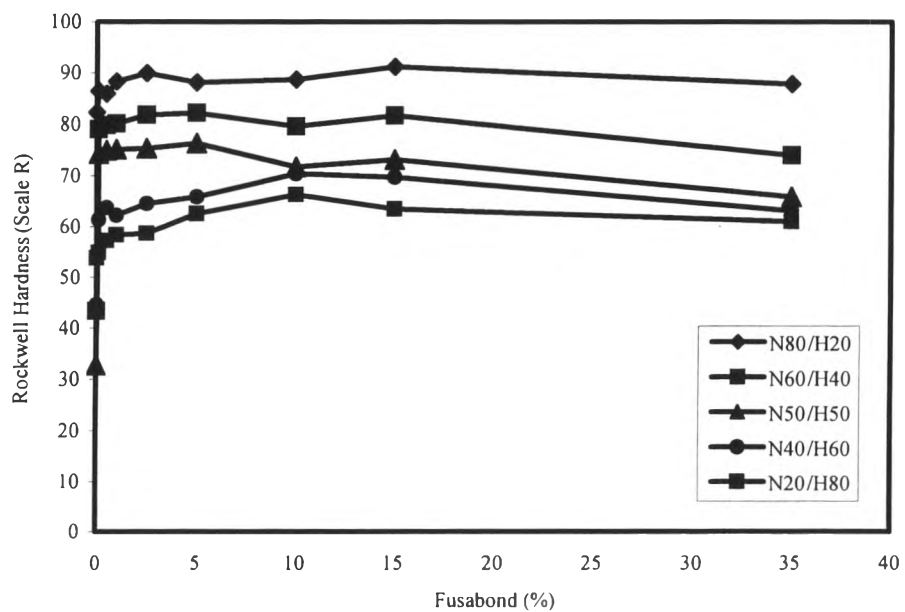


Figure 16 Crystallization temperatures of binary PA6/HDPE blends: (a) pure PA6, (b) 80/20, (c) 60/40, (d) 50/50, (e) 40/60, (f) 20/80, and (g) pure HDPE.

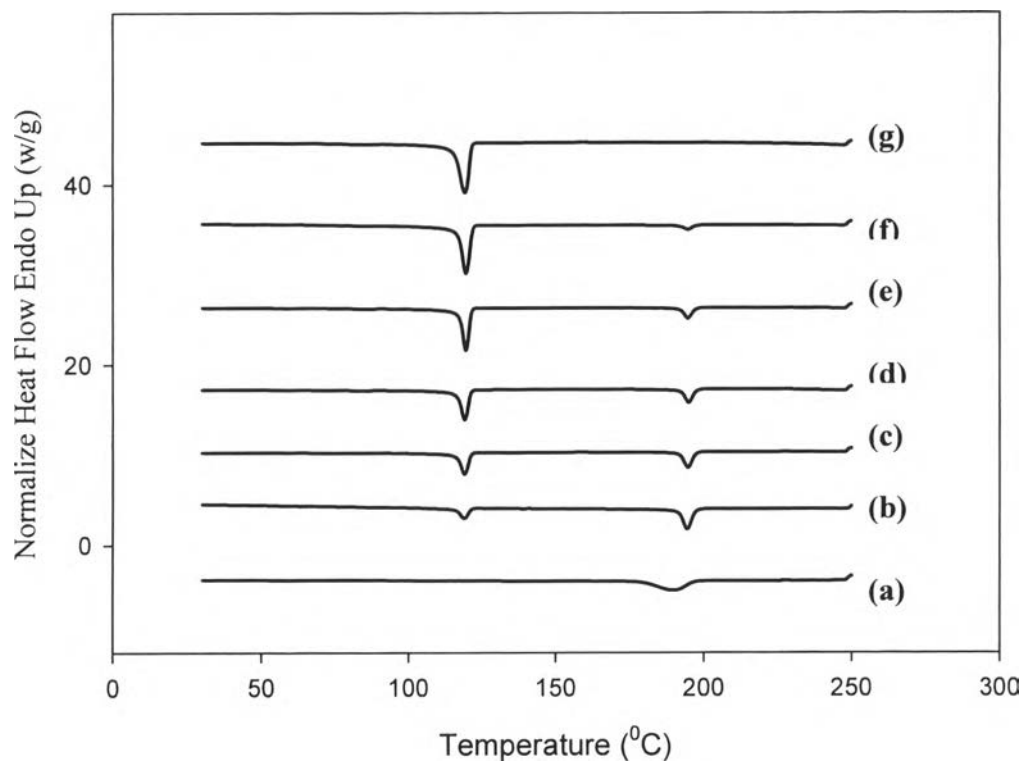


Figure 17 Crystallization temperatures of 80/20 PA6/HDPE blend as a function of Fusabond[®] content: (a) pure HDPE, (b) pure PA6, (c) 0%, (d) 0.1%, (e) 0.5%, (f) 1.0%, (g) 2.5%, (h) 5.0%, (i) 10%, (j) 15%, and (k) 35%

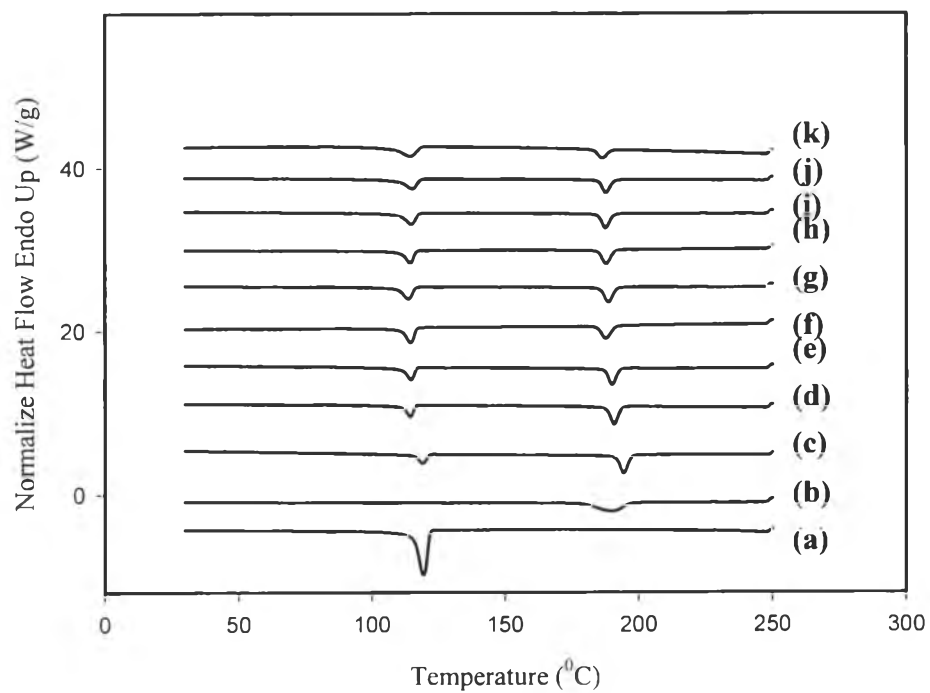


Figure 18 Crystallization temperatures of 20/80 PA6/HDPE blend as a function of Fusabond[®] content: (a) pure HDPE, (b) pure PA6, (c) 0%, (d) 0.1%, (e) 0.5%, (f) 1.0%, (g) 2.5%, (h) 5.0%, (i) 10%, (j) 15%, and (k) 35%.

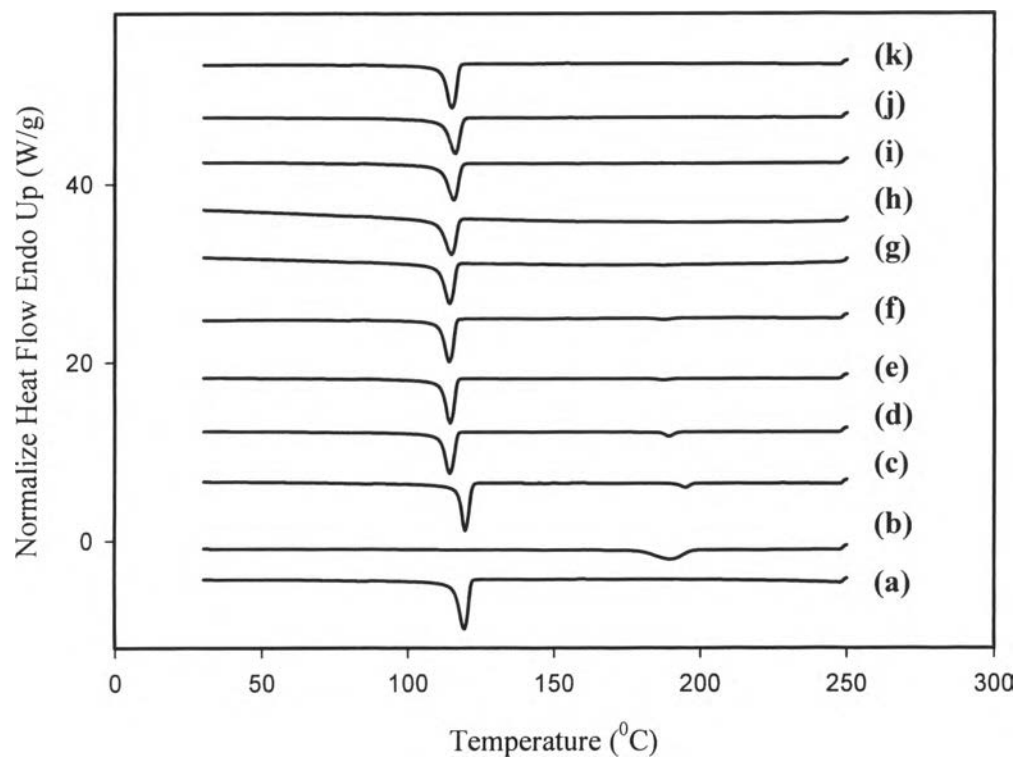


Figure 19 Melting temperatures of binary PA6/HDPE blends: (a) pure PA6, (b) 80/20, (c) 60/40, (d) 50/50, (e) 40/60, (f) 20/80, and (g) pure HDPE.

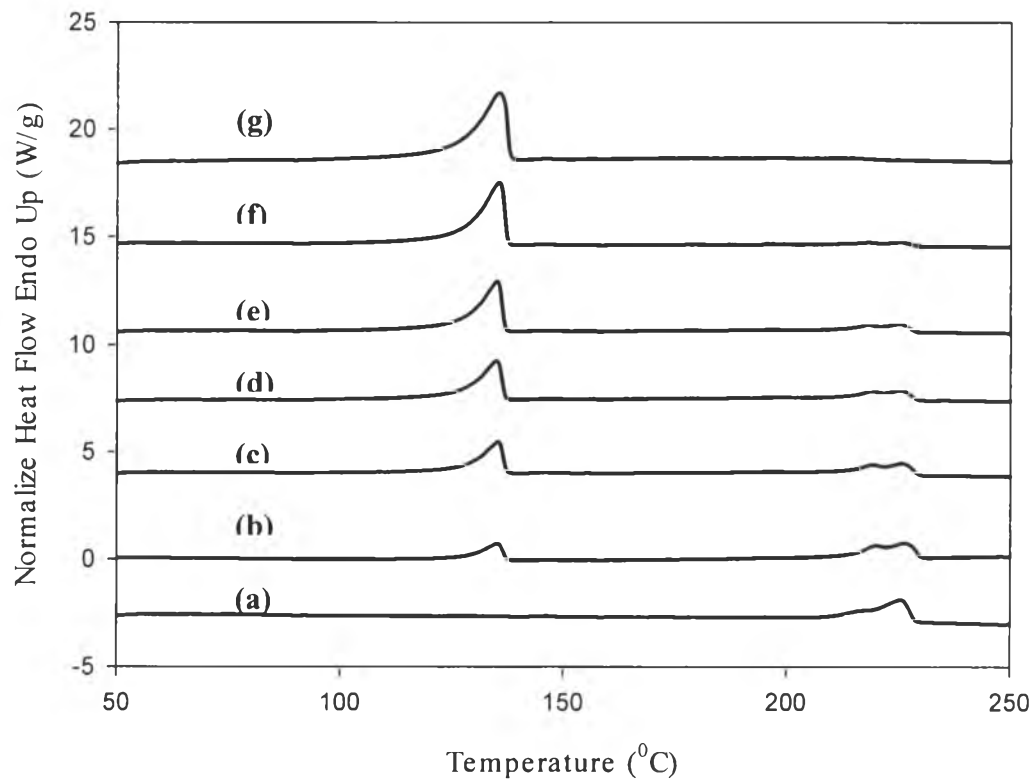


Figure 20 Melting temperatures of 80/20 PA6/HDPE blends as a function Fusabond[®] content: (a) pure HDPE, (b) pure PA6, (c) 0%, (d) 0.1%, (e) 2.5%, (f) 10%, (g) 35%.

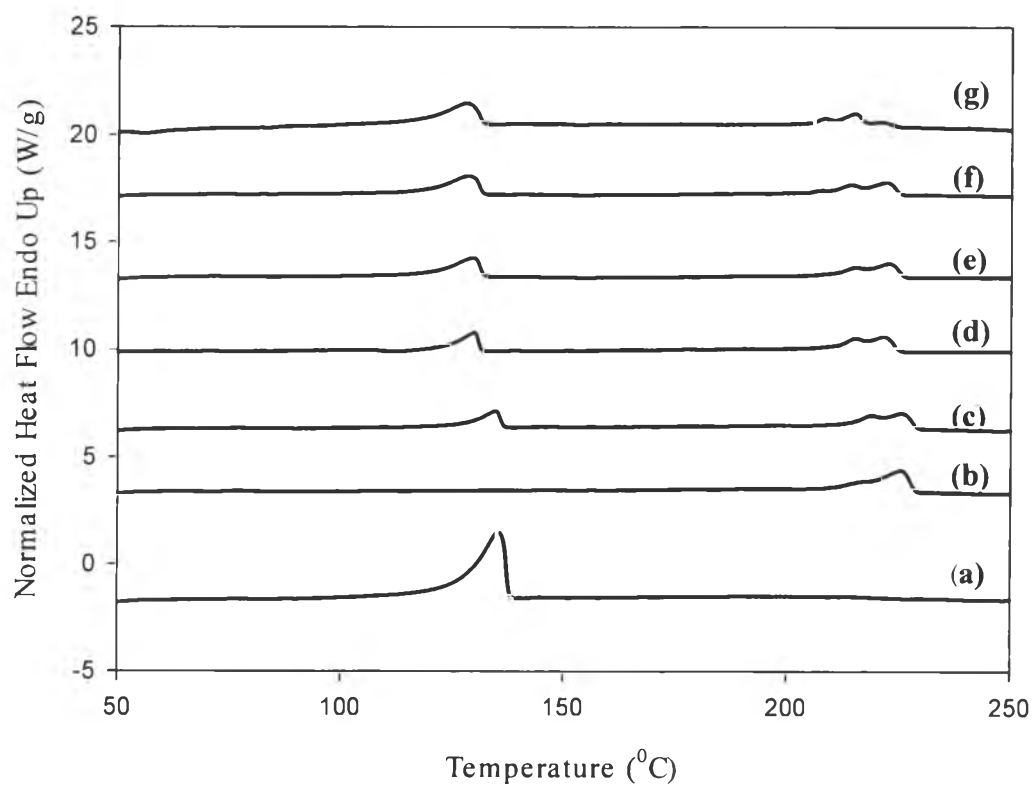


Figure 21 Melting temperatures of 20/80 PA6/HDPE blends as a function Fusabond[®] content: (a) pure HDPE, (b) pure PA6, (c) 0%, (d) 0.1%, (e) 2.5%, (f) 10%, (g) 35%.

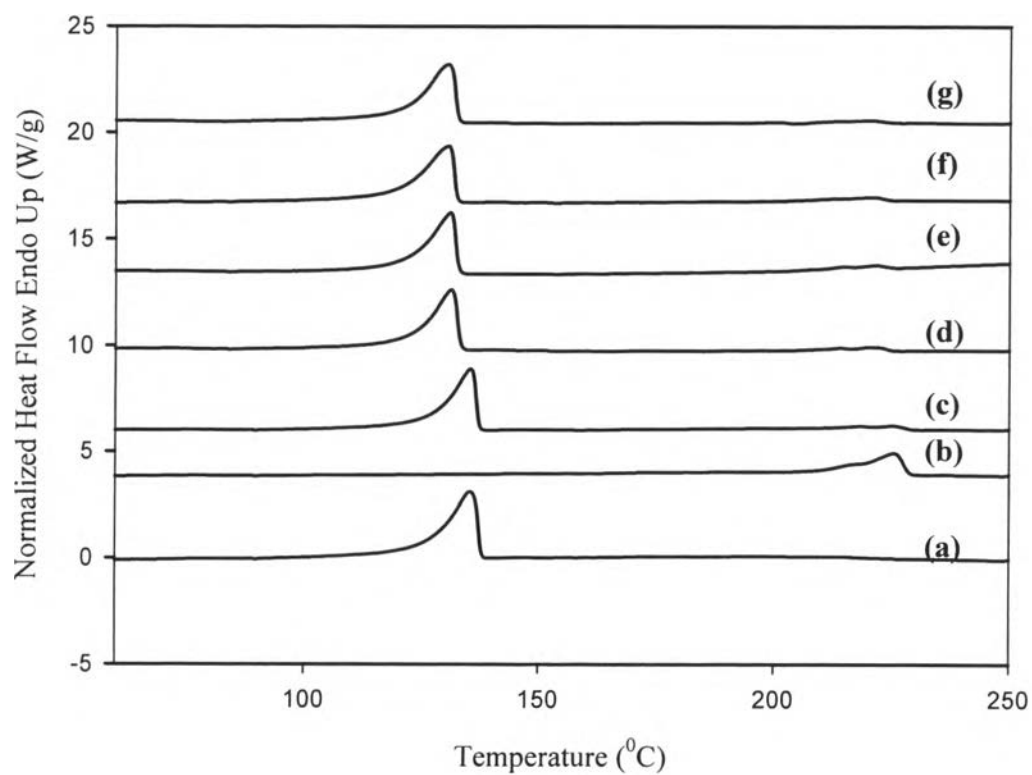


Table 1 The weight fraction of crystallinity of PA6 and HDPE component in PA6/HDPE/Fusabond ternary blends as determined by DSC

Fusabond (% wt.)	PA6/HDPE Ratio									
	80/20		60/40		50/50		40/60		20/80	
	crystallinity of PA6 (%)	crystallinity of HDPE (%)	crystallinity of PA6 (%)	crystallinity of HDPE(%)	crystallinity of PA6 (%)	crystallinity of HDPE(%)	crystallinity of PA6 (%)	crystallinity of HDPE (%)	crystallinity of PA6 (%)	crystallinity of HDPE(%)
0	31.2	41.5	33.3	39.3	34.6	40.4	29.9	42.2	29.5	43.3
0.1	32	44.5	32.6	39.6	37.1	43.9	25.4	45.3	23.8	44
0.5	30.1	49.6	30.7	44.4	32.4	44.7	30.9	42.4	19.3	45.4
1	29.1	65.4	29.2	54.3	28	49.2	25.6	47.5	26.4	45.7
2.5	30	56.6	30.3	52.6	35.4	46	31.4	50.1	28	50.7
5	32.5	54.7	33.8	47.2	34.9	46.1	24.9	45.8	39.3	47.8
10	32.6	52.1	29.7	46.6	30.4	45.8	29.2	46.3	29.9	45.6
15	30.4	45.7	30.6	45.6	30.4	44.8	30.5	44.8	29.4	45.3
35	28.1	40.1	29.2	41.6	32.5	40.5	23.8	44.5	23.2	44.3

Pure PA6 = 35.6%

Pure HDPE = 44.0%

Pure Fusabond = 47.5%

Table 2 Melting and crystallization temperature of PA6 and HDPE components in PA6/HDPE blends with and without Fusabond® as determined by DSC

Blend composition PA6/HDPE/ Fusabond	PA6					HDPE			
	Endothermic			Exothermic		Endothermic		Exothermic	
	T_m (onset)	T_m^{γ}	T_m^{α}	T_c (onset)	T_c	T_m (onset)	T_m	T_c (onset)	T_c
	(°C)	(°C)	(°C)	(°C)	(°C)	(°C)	(°C)	(°C)	(°C)
100/0/0	215.4	217	225.5	196.7	189.8	–	–	–	–
0/100/0	–	–	–	–	–	127.2	135.5	121.6	119.3
0/0/100	–	–	–	–	–	124.5	132	116.8	113.8
80/20/0	212.8	218.7	225.5	197.3	194.5	127.6	134.7	121.4	119
60/40/0	213.7	219	225.7	197.3	194.6	128.2	135.4	121.4	119.1
50/50/0	213.4	219	225.5	197.6	195	127.6	135	121.2	119.1
40/60/0	212.7	218.2	228.4	197.3	194.8	127.4	135	121.4	119.6
20/80/0	209.4	218.9	225.5	197.5	194.8	127.9	135.5	121.9	119.6
80/20/0.1	210.3	215.3	221.7	193.5	190.8	123	129.9	116.2	114.3
60/40/0.1	211.7	216.5	222.2	193.2	190.5	123.6	131	116.5	114.1
50/50/0.1	211.4	215.9	222.4	192.9	190.1	123.5	131	116.6	114.1
40/60/0.1	210.4	215	221.4	192.4	189.8	123.2	131.4	116.9	114.5
20/80/0.1	211.5	215.4	222	192	189.3	123.2	131.2	116.9	114.3
80/20/0.5	206.7	215.6	222.2	192.9	190.1	121.9	130.2	116.7	114.6
60/40/0.5	206.7	215.9	222.2	192.2	189.3	122.5	130.7	116.8	114.6
50/50/0.5	204.6	214.2	221	191.8	189	122.9	130.4	116.8	115
40/60/0.5	205.6	215.2	222	191.7	189.5	122.7	130.9	116.7	114.5
20/80/0.5	209.8	215.7	222	191.1	187.3	122.7	131.2	116.9	114.3
80/20/1.0	204.8	215.7	220.9	191.3	187.8	121.8	130.4	116.7	114.5
60/40/1.0	207	215.9	222.7	192.9	190	122	130.5	116.6	114.1
50/50/1.0	205.8	215	221.7	192.5	189.6	121.4	130	116.7	114.8
40/60/1.0	205.3	215.2	223	192.4	189.5	121.9	130	116.7	114.6
20/80/1.0	208.4	214.9	221.5	191.2	187.5	122	130.9	116.5	114.1
80/20/2.5	205.9	215.6	222.9	191.8	188.8	121	129.7	116.2	113.6
60/40/2.5	206.3	215.2	222.9	192.2	189.1	121.8	130.5	116.6	114.1
50/50/2.5	205.9	215.7	222.4	192.6	189.6	121.5	130.5	117.1	114.8

Blend composition PA6/HDPE/ Fusabond	PA6					HDPE			
	Endothermic			Exothermic		Endothermic		Exothermic	
	T_m (onset)	T_m^{γ}	T_m^{α}	T_c (onset)	T_c	T_m (onset)	T_m	T_c (onset)	T_c
($^{\circ}\text{C}$)	($^{\circ}\text{C}$)	($^{\circ}\text{C}$)	($^{\circ}\text{C}$)	($^{\circ}\text{C}$)	($^{\circ}\text{C}$)	($^{\circ}\text{C}$)	($^{\circ}\text{C}$)	($^{\circ}\text{C}$)	($^{\circ}\text{C}$)
40/60/2.5	204.5	215.8	222.7	192.1	189.1	122.2	131.2	116.7	114.3
2080/2.5	208.9	215	221.9	191.5	187.3	122.2	131.2	116.8	114.1
80/20/5.0	203.8	215	222.4	191.1	187.8	120.6	129.2	116.6	114.3
60/40/5.0	204.1	215.9	222.2	191.4	188.1	121.8	130.5	117.3	114.8
50/50/5.0	205.8	206.2	220.5	191.1	187.8	121.3	130.9	117.1	114.5
40/60/5.0	202.8	215.8	222.2	192.1	187.5	121.3	130.9	117.3	114.8
2080/5.0	206.2	—	222	—	—	120.9	131	117.4	114.8
80/20/10	204.9	214.3	222.2	190.6	187.6	119.4	128	117.6	114.8
60/40/10	204.7	215.3	222.2	190.9	187.6	121.3	130	117.6	115.3
50/50/10	203	214.7	221.9	190.8	187	120.5	130.4	117.8	115.3
40/60/10	201.8	215.8	221.8	192	188.5	120.5	130.5	118.1	115.6
2080/10	207.8	—	221.9	—	—	120.6	130.7	118.4	115.6
80/20/15	205.7	214.9	222.2	190.8	187.8	119.4	128	118	115.1
60/40/15	204.4	214.3	221.9	189.9	186.8	121.1	129.4	118	115.5
50/50/15	204.4	215.4	222.4	191.1	187.5	119.9	129.9	118.2	115.8
40/60/15	202.5	—	221.8	—	—	119.7	130.2	118.9	116
2080/15	207.7	—	220.9	—	—	120.3	130.5	118.8	116.1
80/20/35	205.4	215.2	221.2	189.9	186.5	119	128.2	118.6	114.5
60/40/35	203.1	214.4	221.5	188.2	184.5	120.5	129	118.2	115
50/50/35	206.3	—	221.5	—	—	120.2	131	119.7	115.1
40/60/35	205.9	—	221.5	—	—	120.1	130.5	119.3	115.5
20/80/35	204.1	—	220.9	—	—	122.1	131.2	117.6	115